

Altered dynamic functional connectivity in the default mode network in patients with cirrhosis and minimal hepatic encephalopathy

Hua-Jun Chen¹ · Hai-Long Lin¹ · Qiu-Feng Chen² · Peng-Fei Liu²

Received: 9 January 2017 / Accepted: 4 July 2017 / Published online: 13 July 2017
© Springer-Verlag GmbH Germany 2017

Abstract

Purpose Abnormal brain intrinsic functional connectivity (FC) has been documented in minimal hepatic encephalopathy (MHE) by static connectivity analysis. However, changes in dynamic FC (dFC) remain unknown. We aimed to identify altered dFC within the default mode network (DMN) associated with MHE.

Methods Resting-state functional MRI data were acquired from 20 cirrhotic patients with MHE and 24 healthy controls. DMN seed regions were defined using seed-based FC analysis (centered on the posterior cingulate cortex (PCC)). Dynamic FC architecture was calculated using a sliding time-window method. K-means clustering (number of clusters = 2–4) was applied to estimate FC states.

Results When the number of clusters was 2, MHE patients presented weaker connectivity strengths compared with controls in states 1 and 2. In state 1, decreased FC strength was found between the PCC/precuneus (PCUN) and right medial temporal lobe (MTL)/bilateral lateral temporal cortex (LTC); left inferior parietal lobule (IPL) and right MTL/left LTC; right IPL and right MTL/bilateral LTC; right MTL and right LTC; and medial prefrontal cortex (MPFC) and right MTL/bilateral LTC. In state 2, reduced FC strength was observed between

the PCC/PCUN and bilateral MTL/bilateral LTC; left IPL and left MTL/bilateral LTC/MPFC; and left LTC and right LTC. Altered connectivities from state 1 were correlated with patient cognitive performance. Similar findings were observed when the number of clusters was set to 3 or 4.

Conclusion Aberrant dynamic DMN connectivity is an additional characteristic of MHE. Dynamic connectivity analysis offers a novel paradigm for understanding MHE-related mechanisms.

Keywords Minimal hepatic encephalopathy · Cirrhosis · Dynamic functional connectivity · Default mode network · Resting-state functional magnetic resonance imaging

Abbreviations

MHE	minimal hepatic encephalopathy
HE	hepatic encephalopathy
FC	functional connectivity
DMN	default mode network
dFC	dynamic functional connectivity
HCS	healthy controls
PHES	psychometric hepatic encephalopathy score
MNI	Montreal Neurological Institute
PCC	posterior cingulate cortex
FWE	family-wise error
ROI	region of interest
PCC/PCUN	posterior cingulate cortex/precuneus
MPFC	medial prefrontal cortex
IPL	inferior parietal lobule
MTL	medial temporal lobe
LTC	lateral temporal cortex
ICA	independent component analysis

Electronic supplementary material The online version of this article (doi:10.1007/s00234-017-1881-4) contains supplementary material, which is available to authorized users.

✉ Hua-Jun Chen
chj0075@126.com

¹ Department of Radiology, Fujian Medical University Union Hospital, Fuzhou 350001, China

² School of Information Science and Engineering, Central South University, Changsha 410083, China

Introduction

Minimal hepatic encephalopathy (MHE), which is considered the initial phase in the spectrum of hepatic encephalopathy (HE), is characterized by mild neuropsychological and neurophysiological alterations that are not detectable by routine clinical examination [1]. Despite being a subclinical stage, MHE is considered clinically relevant since it reduces a patient's health-related quality of life, leads to development of overt HE, and is associated with poor outcome [2–4].

Resting-state fMRI studies have demonstrated that MHE patients show altered brain intrinsic functional connectivity (FC), which plays an important role in MHE-related mechanisms. For example, significant FC reduction within the default mode network (DMN) has been revealed in cirrhotic patients with MHE and is associated with cognitive impairment as well as HE development [5]. Furthermore, a correlation was observed between disrupted DMN connectivity and hyperammonemia, which is the core neuropathophysiology of MHE [6]. In addition to abnormalities in the DMN, altered FC has been observed in many other brain intrinsic networks such as attention and visual networks [7]. Also, altered topological properties of whole-brain networks have been revealed in MHE [8].

Although these studies have greatly advanced our understanding of changes in the large-scale functional organization of the brain in MHE, it is notable that all previous findings were obtained using traditional resting-state connectivity analysis, which is based on the implicit assumption that FC during the recording period is relatively static. However, this assumption of stationarity is inconsistent with the fact that the brain is highly dynamic [9]. For example, temporal variations in brain intrinsic FC have been demonstrated by an increasing number

of task-related and resting-state functional MRI studies [9, 10]. Thus, static connectivity analysis is not sufficient to evaluate brain functions in both healthy and diseased cases.

Recently, increasing attention has focused on time-varying properties of brain FC. These studies have yielded promising results for extending our understanding of brain function [10, 11] and exploring the neural bases of dysfunction in several neuropsychological diseases such as Alzheimer's disease [12], schizophrenia [13], and epilepsy [14]. However, the dynamic FC (dFC) characteristics remain largely unknown in MHE patients. In this study, we aimed to identify changes in dFC within the DMN in cirrhotic patients with MHE, which may provide new insight into MHE-related pathophysiology.

Subjects and methods

Participants

This study included 20 cirrhotic patients with MHE and 24 healthy controls (HCs) (Table 1). The psychometric hepatic encephalopathy score (PHES) examination, including digit symbol test, number connection test A, number connection test B, serial dotting test, and line tracing test, was used for the diagnosis of MHE. A detailed description of PHES tests and criteria for defining MHE has been described previously [15]. The subjects with current overt HE or other neuropsychiatric disorders and those taking psychotropic medications, suffering from uncontrolled endocrine or metabolic diseases, or with a history of alcohol abuse during the 6 months prior to the study were excluded. This study was approved by the local Medical Research Ethics Committee. All participants provided written informed consent before the study.

Table 1 Demographic and clinical characteristics of the subjects

	HC subjects (<i>n</i> = 24)	MHE patients (<i>n</i> = 20)	<i>P</i> value
Age (year)	50.9 ± 7.0	49.4 ± 9.1	0.540
Gender (male/female)	18/6	15/5	NS
Education level (year)	8.7 ± 2.6	8.5 ± 2.8	0.768
Etiology of cirrhosis (HBV/alcoholism/HBV + alcoholism/other)	-	12/3/1/4	-
Child-Pugh stage (A/B/C)	-	4/12/4	-
PHES tests			
Final PHES (score)	0.6 ± 2.1	-7.5 ± 2.0	<0.001
Number connection test A (seconds)	36.2 ± 12.2	57.0 ± 14.9	<0.001
Number connection test B (seconds)	61.8 ± 28.9	120.3 ± 47.8	<0.001
Serial dotting test (s)	42.7 ± 7.3	59.2 ± 8.8	<0.001
Digit symbol test (raw score)	44.9 ± 8.9	28.8 ± 8.5	<0.001
Line tracing test (raw score)	113.4 ± 16.6	183.4 ± 37.1	<0.001

MHE minimal hepatic encephalopathy, HC healthy control, NS not significant, PHES psychometric hepatic encephalopathy score, HBV hepatitis B virus

MRI data acquisition

All MRI data were acquired on a 3.0 T scanner (Siemens, Verio, Germany). Resting-state functional images were acquired using an echo planar imaging sequence with the following parameters: 35 contiguous axial slices, TR = 2000 ms, TE = 25 ms, FOV = 240 mm × 240 mm, matrix = 64 × 64, flip angle = 90°, and slice thickness = 4 mm. Participants were instructed to keep their eyes closed, not think of anything in particular, and keep their heads still. In addition, three-dimensional T1-weighted magnetization-prepared rapid gradient echo (MPRAGE) sagittal images were collected using the following parameters: TR = 1.9 ms, TE = 2.48 ms, FOV = 256 mm × 256 mm, matrix = 256 × 256, flip angle = 9°, slice thickness = 1.0 mm, 176 slices.

Functional image preprocessing

Functional data were preprocessed using SPM software and the Data Processing Assistant for Resting-State fMRI (DPARSF, <http://www.restfmri.net/forum/DPARSF>) tool. The first 10 volumes were discarded to allow for scanner calibration and adaptation of the participants to the scanning environment. Slice-timing adjustment and realignment for head-motion correction were performed. Subjects with more than 2-mm maximum displacement in any of the *x*-, *y*-, or *z*-directions or more than 2.0° angular rotation about any axis would have been excluded from the study; however, no participant was excluded. There were no significant differences regarding translational or rotational movements in any direction between the two groups. The individual structural image (T1-weighted MPRAGE images) was coregistered to the mean functional image after motion correction. The transformed structural images were then segmented into gray matter, white matter, and cerebrospinal fluid using a unified segmentation algorithm. The motion corrected functional volumes were spatially normalized to the Montreal Neurological Institute (MNI) space and resampled to 3-mm isotropic voxels using the normalization parameters estimated during unified segmentation. Finally, the functional images were smoothed using a Gaussian filter with full-width at half-maximum of 8 mm. Any linear trend was then removed. The resulting fMRI data were band-pass filtered (0.01–0.08 Hz) to reduce low-frequency drift as well as high-frequency physiological respiratory and cardiac noise. Considering the possible effects of head motion as well as global, white matter, and cerebrospinal fluid signals on the results, we also removed several sources of spurious variance by linear regression, which included six head motion parameters and average signals from cerebrospinal fluid, white matter, and the whole brain.

Definition of DMN seed regions

A seed-based connectivity analysis was performed to identify the DMN pattern. The seed was centered on the bilateral posterior cingulate cortex (PCC; MNI coordinates: $x = 0, y = -53, z = 26$) [6] with a radius of 6 mm. The mean time series of the PCC seed was extracted as the reference time course, and cross-correlation analysis was then conducted between the mean time course of the PCC and the time series of every voxel of the whole brain. Finally, a Fisher's *z*-transform was applied to improve normality of the correlation coefficients.

The individual correlation maps from the control group were subjected to a random-effect analysis by using a one-sample *t* test. The threshold was set at $P < 0.05$, family-wise error (FWE) corrected. The major nodes of the DMN map from the control group were then defined as the DMN seed regions (region of interest, ROI), which included the PCC/precuneus (PCUN), medial prefrontal cortex (MPFC), bilateral inferior parietal lobule (IPL), medial temporal lobe (MTL), and lateral temporal cortex (LTC). The selection of DMN seed regions was based on previous studies on DMN anatomical and functional locations [6, 16]. Characteristics of the DMN seed regions are presented in Fig. 1 and Table 2.

Computation of dFC within the DMN

The dynamic brain connectome analysis toolbox (<http://restfmri.net/forum/DynamicBC>) was used to compute dFC within the DMN. We initially extracted representative signals of DMN ROIs for each subject and then calculated dFC changes using a sliding time-window correlation

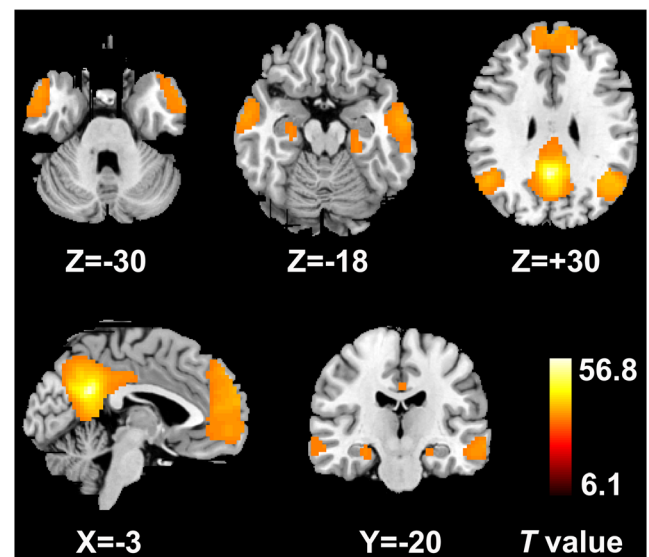


Fig. 1 Eight regions of interest (ROIs) within the DMN. These ROIs were derived from the DMN map of healthy controls and include the posterior cingulate cortex/precuneus, medial prefrontal cortex, bilateral inferior parietal lobule, bilateral medial temporal lobe, and bilateral lateral temporal cortex

Table 2 Characteristics of the seed regions within the DMN map of healthy controls

DMN regions	Cluster size (voxels)	Brodmann's area	MNI coordinates (mm)			Peak <i>t</i> value
			<i>x</i>	<i>y</i>	<i>z</i>	
PCC/PCUN	1473	31/7/23/30/29	3	−54	27	56.88
l-IPL	448	39/40	−45	−57	30	17.46
r-IPL	285	39/40	48	−57	27	15.24
l-MTL	57	35/36	−21	−33	−12	9.39
r-MTL	33	35/36	27	−18	−18	7.85
l-LTC	481	20/21	−60	−9	−18	12.88
r-LTC	333	20/21	54	12	−33	12.28
MPFC	1834	10/9/8/32	−3	63	18	15.45

PCC/PCUN posterior cingulate cortex/precuneus, *IPL* inferior parietal lobule, *MTL* medial temporal lobe, *LTC* lateral temporal cortex, *MPFC* medial prefrontal cortex

The letters “l” and “r” indicate left and right side, respectively. These brain regions were selected as the regions of interest (ROIs) within the DMN during dynamic connectivity analysis

(SWC) method. We computed correlations between every pair of ROIs using a sliding temporal window, with a width of 20 TRs (40 s) slid in steps of 1 TR (2 s). We set the width of each window to 20 TRs according to previous studies [9, 11, 17–20]. For each sliding window, we obtained a correlation matrix (across 8 DMN ROIs), which was then converted to *z*-scores using the Fisher *r*-to-*z* transformation. To test the effect of different time-window length on the result, we also set window size at 50 TRs (100 s) and investigated the dynamic functional connectivity in DMN across two groups, given that recent studies have suggested that the spurious correlations of the SWC result are reduced when the size of the window is greater than $1/f_{\min}$ (f_{\min} = minimum frequency) [21]. The SWC results (with time-window length = 100 s) see supplementary materials.

Identification of connectivity states

Given that FC patterns reoccur across windows and subjects, we initially applied *K*-means clustering to extract the common (group-level) FC states [22] and then estimated the subject-specific FC states. In each state, we then examined between-group differences with respect to connectivity strength based on subject-specific FC states. *K*-mean clustering was performed over a range of cluster sizes ($K = 2$ –4) and revealed similar FC states (see Supplementary Fig. 1 and Supplementary Fig. 2). We displayed the results of the *K*-means clustering method with the number of clusters = 2. Based on the subject-specific states corresponding to the same group-level state, two-sample two-tailed *t* tests were performed to test group differences in connectivity strength.

Also, we examined between-group difference with respect to the dwell time in each state and the transition times between states, by using two-sample two-tailed *t* tests. For each subject, the dwell time in each state is regarded as the number of

windows belonging to this state related cluster [23]. Meanwhile, the transition times between states were recorded for each subject and compared across two groups.

Correlation between connectivity strength from different states and cognitive performance

Altered connectivities in states 1 and 2 were extracted. Then, the Spearman correlation analyses were performed between connectivity strength and PHES result in MHE patients. $P < 0.05$ was considered statistically significant.

Results

Figure 2 shows the common states (matrix) of FC across DMN regions, which were extracted using the *K*-means clustering method with cluster size = 2. The visualized network patterns of the common FC states were obtained at a threshold of 0.35 to highlight differences in connectivity pattern between the 2 states. State 1 exhibited stronger connectivity strengths across 8 DMN regions relative to state 2. In addition, we set the number of clusters to 3 and 4 when *K*-means clustering was performed, and similar results were observed (see Supplementary Fig. 3 and Supplementary Fig. 4).

Figure 3 shows the between-group difference in dFC within the DMN. By comparing subject-specific states, we found a significant reduction in FC of MHE patients during both states 1 and 2, while no increased connectivity was found in MHE patients. In state 1, MHE patients showed significantly decreased connectivity strength along 12 connections, which included PCC/PCUN, right MTL; PCC/PCUN, left LTC; PCC/PCUN, right LTC; left IPL, right MTL; left IPL, left LTC; right IPL, right MTL; right IPL, left LTC; right IPL, right LTC; right MTL, right LTC; right MTL, MPFC; left

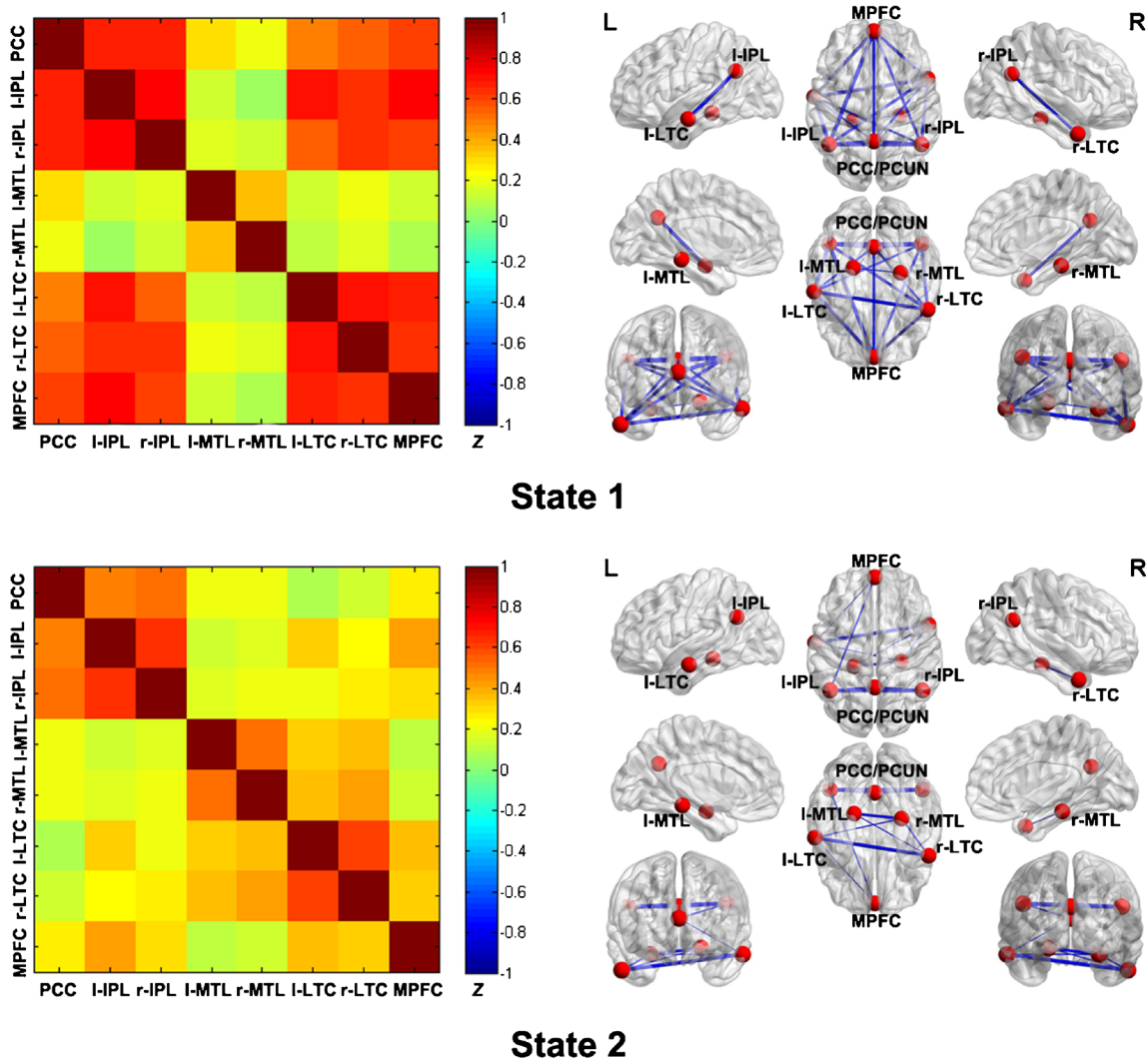


Fig. 2 The common states (matrix) of functional connectivity within the DMN, which was extracted using the *K*-means clustering method, and the visualized network pattern of the common functional connectivity states

LTC, MPFC; and right LTC, MPFC. Among these 12 connections, 10 remained significantly reduced connectivity strength in the MHE group, after the correction for multiple comparisons by false-discovery rate (FDR) procedure. Details on decreased connectivity in state 1 are summarized in Table 3. In state 2, reduced connectivity strength was observed along 9 connections, which included PCC/PCUN, left MTL; PCC/PCUN, right MTL; PCC/PCUN, left LTC; PCC/PCUN, right LTC; left IPL, left MTL; left IPL, left LTC; left IPL, right LTC; left IPL, MPFC; and left LTC, right LTC. Among these 9 connections, only 1 remained significantly reduced connectivity strength in the MHE group, after the correction for multiple comparisons by FDR procedure. Details on decreased connectivity in state 2 are summarized in Table 4. In addition, when the number of clusters was set to 3 or 4 (with window size = 40 s), similar results in two-sample *t* tests were observed (see Supplementary Fig. 3 and Supplementary Fig. 4).

at a threshold of 0.35. The line sizes indicate functional connectivity strength in the states

Meanwhile, when the window size was set at 100 s (with cluster number = 2), the similar findings were also obtained (see Supplementary Fig. 5 and Supplementary Fig. 6). In summary, compared with HCs, MHE patients presented weaker connectivity strengths in both states 1 and 2.

Based on the between-group comparison of the dwell time in states, we found that MHE patients seemed to stay in state 2 (in which the subsystems of DMN were less connected) for the longer time, compared with healthy controls (Fig. 4). But this trend did not reach statistically significant level ($P = 0.138$). No significant difference in transition times was found between two groups ($P = 0.474$), which may suggest the similarity in the variability of the functional network dynamics across two groups, to some extent.

In MHE patients, several altered connectivities in state 1, including PCC/PCUN, right MTL; left IPL, right MTL; right IPL, right MTL; right IPL, right LTC; and right MTL, MPFC,

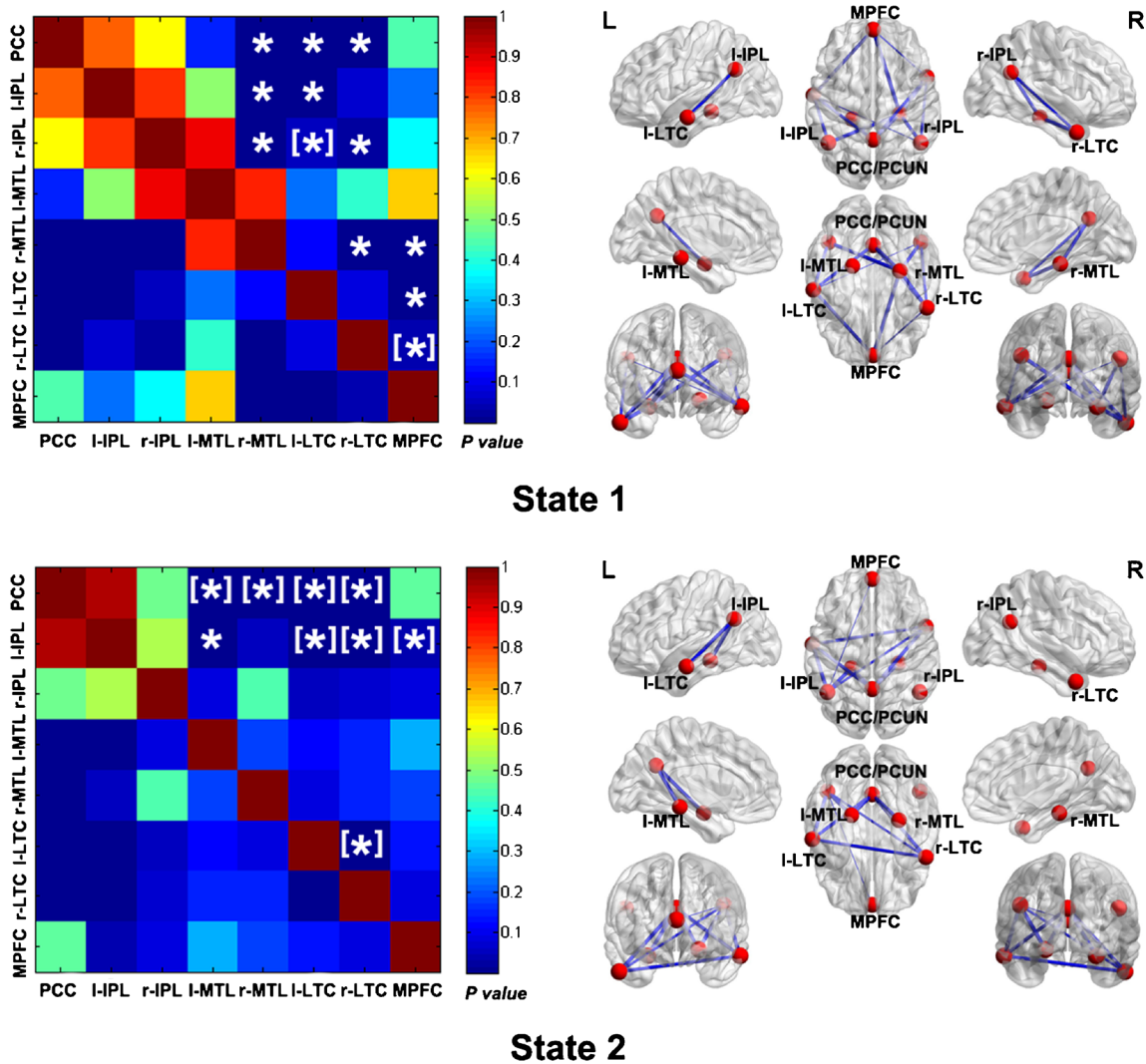


Fig. 3 The two-sample *t* test results from comparing subject-specific functional connectivity states between the 2 groups and visualized aberrant connectivities for states 1 and 2. The line sizes indicate significance of between-group differences in functional connectivity.

The “*” denotes significantly decreased connectivity ($P < 0.05$, FDR corrected) in the patient group. The “[*]” denotes significantly decreased connectivity ($P < 0.05$, uncorrected) in the patient group

were correlated with PHES result (Table 5). Figure 5 shows the significant correlation between connectivity strength (along 4 connections, see Table 5) and PHES result, after the correction for multiple comparisons by FDR procedure. In state 2, no significant correlation was observed between connectivity strength and PHES result.

Discussion

Recent studies have highlighted characteristics of dFC in the human brain, which has attracted increasing attention [9, 10]. Consistent with these reports, we found different FC states of the DMN in both HCs and MHE patients; a stronger connectivity pattern across DMN regions was clearly observed in

several states when compared with the other states. Furthermore, by comparing subject-specific FC states, we found that MHE patients presented weaker DMN connectivity strengths compared with HCs in all functional states. The DMN is considered a major contributor to normal cognitive functions such as attention and executive functions [16, 24]. Therefore, lower DMN connectivity might suggest cognitive impairment due to MHE. This implication is supported by the results of correlation analysis, which showed that altered dFC was significantly correlated with patients’ cognitive performance assessed by the PHES test. These findings further confirmed the essential role of DMN dysfunction in MHE mechanisms.

By utilizing various static connectivity analysis methods, such as independent component analysis (ICA) and seed-

Table 3 Significant reduction of dynamic functional connectivity within the DMN (state 1) in MHE patients compared with healthy controls

Connectivity	Connectivity strength (Z value)		P value
	HC subjects	MHE patients	
PCC/PCUN-r-MTL	0.236 ± 0.217	−0.003 ± 0.204	0.0005#
PCC/PCUN-l-LTC	0.480 ± 0.140	0.342 ± 0.205	0.0116#
PCC/PCUN-r-LTC	0.528 ± 0.173	0.385 ± 0.202	0.0154#
l-IPL-r-MTL	0.121 ± 0.221	−0.081 ± 0.207	0.0033#
l-IPL-l-LTC	0.696 ± 0.140	0.555 ± 0.215	0.0122#
r-IPL-r-MTL	0.183 ± 0.194	0.001 ± 0.223	0.0058#
r-IPL-l-LTC	0.532 ± 0.175	0.409 ± 0.227	0.0484
r-IPL-r-LTC	0.641 ± 0.124	0.508 ± 0.223	0.0164#
r-MTL-r-LTC	0.279 ± 0.205	0.075 ± 0.221	0.0029#
r-MTL-MPFC	0.172 ± 0.192	−0.086 ± 0.232	0.0002#
l-LTC-MPFC	0.697 ± 0.102	0.532 ± 0.260	0.0065#
r-LTC-MPFC	0.629 ± 0.130	0.510 ± 0.230	0.0370

PCC/PCUN posterior cingulate cortex/precuneus, IPL inferior parietal lobule, MTL medial temporal lobe, LTC lateral temporal cortex, MPFC medial prefrontal cortex

The letters “l” and “r” indicate left and right side, respectively. The “#” indicates statistical significance ($P < 0.05$), after correction for multiple comparisons by false-discovery rate (FDR) procedure

based connectivity approach, many studies have consistently revealed a reduction of DMN FC in MHE patients [5, 6, 25, 26]. Our results showed decreased DMN dFC, which extends existing findings and further verifies loss of DMN integrity in MHE. According to previous studies, DMN dysfunction

Table 4 Significant reduction of dynamic functional connectivity within the DMN (state 2) in MHE patients compared with healthy controls

Connectivity	Connectivity strength (Z value)		P value
	HC subjects	MHE patients	
PCC/PCUN-l-MTL	0.445 ± 0.274	0.175 ± 0.263	0.0018
PCC/PCUN-r-MTL	0.436 ± 0.282	0.173 ± 0.235	0.0019
PCC/PCUN-l-LTC	0.347 ± 0.276	0.085 ± 0.310	0.0051
PCC/PCUN-r-LTC	0.397 ± 0.282	0.114 ± 0.311	0.0029
l-IPL-l-MTL	0.329 ± 0.249	0.042 ± 0.258	0.0006#
l-IPL-l-LTC	0.594 ± 0.225	0.332 ± 0.282	0.0013
l-IPL-r-LTC	0.457 ± 0.267	0.247 ± 0.285	0.0158
l-IPL-MPFC	0.572 ± 0.206	0.418 ± 0.254	0.0320
l-LTC-r-LTC	0.615 ± 0.159	0.608 ± 0.141	0.0071

PCC/PCUN posterior cingulate cortex/precuneus, IPL inferior parietal lobule, MTL medial temporal lobe, LTC lateral temporal cortex, MPFC medial prefrontal cortex

The letters “l” and “r” indicate left and right side, respectively. The “#” indicates statistical significance ($P < 0.05$), after correction for multiple comparisons by false-discovery rate (FDR) procedure

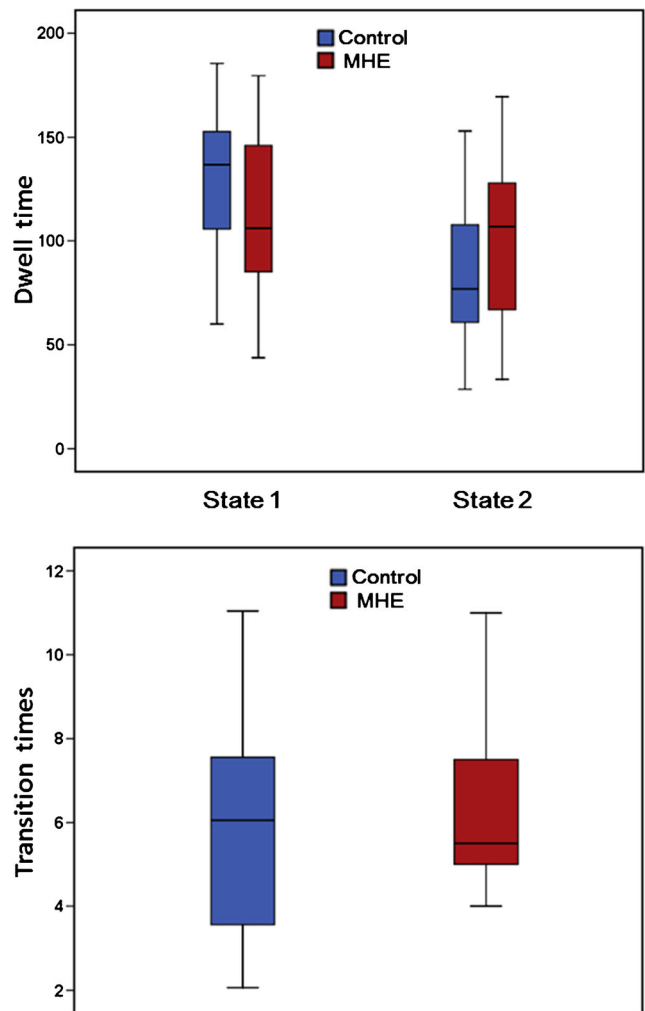


Fig. 4 The between-group comparison of the dwell time in states and transition times. The boxplots show the dwell time and transition times in healthy controls (blue) and MHE patients (red). MHE patients seemed to spend longer time to stay in state 2, compared with healthy controls. But this trend did not reach statistically significant level ($P = 0.138$). No significant difference in transition times was found between two groups ($P = 0.474$)

Table 5 The correlation between cognitive performance and dynamic functional connectivity within the DMN (state 1) in MHE patients

Connectivity	r value	P value	Connectivity	r value	P value
PCC/PCUN-r-MTL	0.581	0.007#	r-IPL-l-LTC	0.403	0.078
PCC/PCUN-l-LTC	0.203	0.391	r-IPL-r-LTC	0.674	0.001#
PCC/PCUN-r-LTC	0.225	0.340	r-MTL-r-LTC	0.407	0.075
l-IPL-r-MTL	0.535	0.015#	r-MTL-MPFC	0.506	0.023
l-IPL-l-LTC	0.363	0.115	l-LTC-MPFC	0.269	0.251
r-IPL-r-MTL	0.571	0.009#	r-LTC-MPFC	0.315	0.176

PCC/PCUN posterior cingulate cortex/precuneus, IPL inferior parietal lobule, MTL medial temporal lobe, LTC lateral temporal cortex, MPFC medial prefrontal cortex

The letters “l” and “r” indicate left and right side, respectively. The “#” indicates statistical significance ($P < 0.05$), after correction for multiple comparisons by false-discovery rate (FDR) procedure

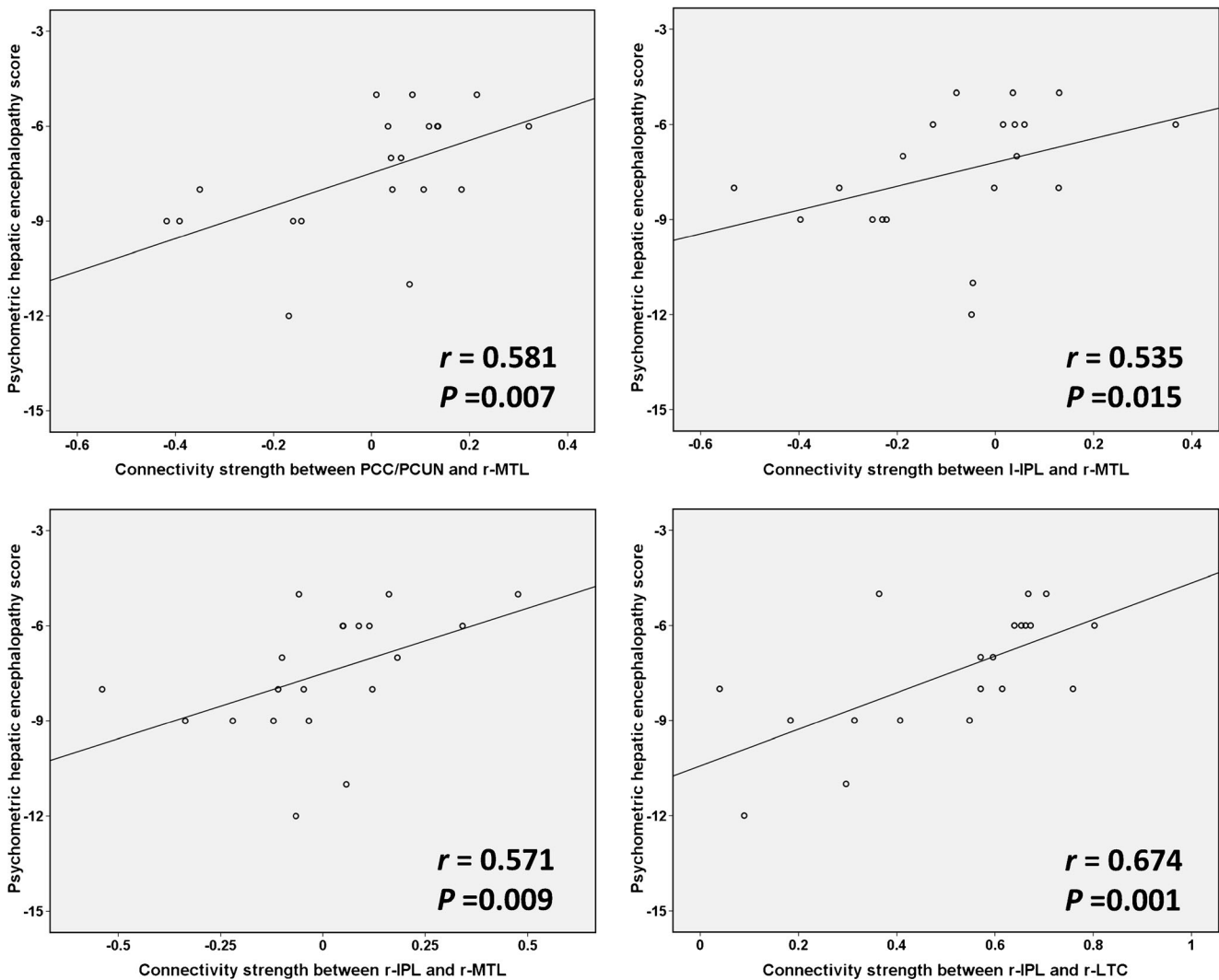


Fig. 5 The correlation between functional connectivity strength in state 1 and cognitive test result. The connectivity strength along 4 connections is found to be correlated with PHEs result, after the correction for multiple comparisons by FDR procedure

(reflected by altered FC) may be associated with several pathological processes in cirrhosis such as inhibition of cerebral energy metabolism involving DMN-related regions [27] and cerebral edema attributed to metabolic disturbance of ammonia [25].

Previous resting-state functional MRI studies have demonstrated that several DMN regions such as the PCC/PCUN show remarkably decreased connectivity with other regions [5, 25, 26]. Consistent with these results, our dynamic connectivity analysis showed significantly reduced connectivity from the PCC/PCUN to the MTL and LTC, regardless of whether the data were obtained during functional state 1 or 2. This finding further suggests that the PCC/PCUN is preferentially vulnerable during MHE. This implication is well supported by structural neuroimaging studies revealing that the PCC/PCUN region undergoes dramatic morphological atrophy due to cirrhosis and its complications (HE) [28, 29]. Of

note, several previous studies have suggested that a disrupted connection between anterior and posterior DMN components (e.g., PCC/PCUN to MPFC) is an important characteristic in cirrhotic patients without overt HE [26, 28]; however, this was not observed in our study. The conflicting results may be attributed to different data processing methods: we used a ROI-wise correlation analysis, while the other studies used a voxel-wise correlation approach. It is worth noting that another study utilizing a ROI-wise correlation method found no significant change in connectivity between the PCC/PCUN and MPFC [6], which may verify the reliability of our result.

In studies using static connectivity analysis, the MPFC is another area that often shows decreased connections with other DMN regions such as the hippocampal formation, temporal pole, and inferior parietal cortex [6]. Consistent with these results, we found decreased connections between the MPFC-MTL and MPFC-LTC in state 1 and MPFC-IPL in state 2. It is

notable that our findings may indicate MHE-related changes in MPFC connectivity patterns associated with different functional conditions of the DMN that cannot be detected by static connectivity analysis. In addition, reduced connectivity along the IPL-LTC and IPL-MTL pathways was observed in MHE patients. These findings are not well described by previous studies, although group-ICA studies have suggested decreased FC in the bilateral angular gyrus and parahippocampal gyrus [7]. This phenomenon may be attributed to the limited ability of conventional static connectivity analysis to capture time-varying properties of brain network connectivity. Based on the advantage of dynamic FC analysis, we could explore MHE-related FC alteration more comprehensively.

Several limitations of the current study should be addressed. First, the relatively small sample size may reduce the generalizability of our results to some extent. Second, we only examined alterations of dynamic connectivity within the DMN. Further studies must examine, in more detail, dFC changes within or between other brain intrinsic networks, such as attention and salience networks, that are affected by MHE. Third, we investigated MHE-related changes in FC strength (functional coupling between different DMN ROIs) within distinct states. Other time-varying connectivity metrics (e.g., graph metrics) should be examined in future studies to provide more comprehensive insight into dFC characteristics in MHE. Fourth, we applied the sliding window correlation, whose performance depends on the choice of multiple parameters [30]. For example, the frequency components of the fMRI signal and the window size interact to affect the introduction of spurious correlations [18, 20]. Thus, more comprehensive study is recommended to validate our findings, by using distinct fMRI data and parameter setting, in the future. Fifth, future longitudinal studies are recommended to define the evolution of DMN dynamic connectivity during progression of HE and following various therapies, to validate the potential of altered dynamic connectivity as a clinical biomarker.

In conclusion, aberrant dynamic DMN connectivity is an additional characteristic of MHE. Disruption of DMN integrity in MHE is associated with patient cognitive impairment. Dynamic connectivity analysis offers a novel paradigm for understanding mechanisms underlying MHE.

Compliance with ethical standards

Funding This work was funded by a grant from the National Natural Science Foundation of China (No. 81501450) and a project funded by the China Postdoctoral Science Foundation (No. 2015M580452).

Conflict of interest The authors declare that they have no conflict of interest.

Ethical approval All procedures performed in the studies involving human participants were in accordance with the ethical standards of the Medical Research Ethics Committee of Fujian Medical University Union

Hospital and/or national research committee and with the 1964 Helsinki Declaration and its later amendments or comparable ethical standards.

Informed consent Informed consent was obtained from all individual participants included in the study.

References

- Bajaj JS, Wade JB, Sanyal AJ (2009) Spectrum of neurocognitive impairment in cirrhosis: implications for the assessment of hepatic encephalopathy. *Hepatology* 50:2014–2021
- Romero-Gomez M, Boza F, Garcia-Valdecasas MS, Garcia E, Aguilar-Reina J (2001) Subclinical hepatic encephalopathy predicts the development of overt hepatic encephalopathy. *Am J Gastroenterol* 96:2718–2723
- Groeneweg M, Quero JC, De Bruijn I et al (1998) Subclinical hepatic encephalopathy impairs daily functioning. *Hepatology* 28: 45–49
- Dhiman RK, Kurmi R, Thumburu KK et al (2010) Diagnosis and prognostic significance of minimal hepatic encephalopathy in patients with cirrhosis of liver. *Dig Dis Sci* 55:2381–2390
- Chen HJ, Jiao Y, Zhu XQ et al (2013) Brain dysfunction primarily related to previous overt hepatic encephalopathy compared with minimal hepatic encephalopathy: resting-state functional MR imaging demonstration. *Radiology* 266:261–270
- Qi R, Zhang LJ, Xu Q et al (2014) Abnormal functional connectivity within the default mode network in patients with HBV-related cirrhosis without hepatic encephalopathy revealed by resting-state functional MRI. *Brain Res* 1576:73–80
- Qi R, Zhang LJ, Xu Q et al (2012) Selective impairments of resting-state networks in minimal hepatic encephalopathy. *PLoS One* 7: e37400
- Hsu TW, Wu CW, Cheng YF et al (2012) Impaired small-world network efficiency and dynamic functional distribution in patients with cirrhosis. *PLoS One* 7:e35266
- Hutchison RM, Womelsdorf T, Allen EA et al (2013) Dynamic functional connectivity: promise, issues, and interpretations. *NeuroImage* 80:360–378
- Calhoun VD, Miller R, Pearlson G, Adali T (2014) The chronnectome: time-varying connectivity networks as the next frontier in fMRI data discovery. *Neuron* 84:262–274
- Allen EA, Damaraju E, Plis SM, Erhardt EB, Eichele T, Calhoun VD (2014) Tracking whole-brain connectivity dynamics in the resting state. *Cereb Cortex* 24:663–676
- Jones DT, Vemuri P, Murphy MC et al (2012) Non-stationarity in the "resting brain's" modular architecture. *PLoS One* 7:e39731
- Rashid B, Damaraju E, Pearlson GD, Calhoun VD (2014) Dynamic connectivity states estimated from resting fMRI identify differences among schizophrenia, bipolar disorder, and healthy control subjects. *Front Hum Neurosci* 8:897
- Liao W, Zhang Z, Mantini D et al (2014) Dynamical intrinsic functional architecture of the brain during absence seizures. *Brain Struct Funct* 219:2001–2015
- Chen HJ, Jiang LF, Sun T, Liu J, Chen QF, Shi HB (2015) Resting-state functional connectivity abnormalities correlate with psychometric hepatic encephalopathy score in cirrhosis. *Eur J Radiol* 84: 2287–2295
- Buckner RL, Andrews-Hanna JR, Schacter DL (2008) The brain's default network: anatomy, function, and relevance to disease. *Ann N Y Acad Sci* 1124:1–38
- Li X, Zhu D, Jiang X et al (2014) Dynamic functional connectomics signatures for characterization and differentiation of PTSD patients. *Hum Brain Mapp* 35:1761–1778

18. Shirer WR, Ryali S, Rykhlevskaia E, Menon V, Greicius MD (2012) Decoding subject-driven cognitive states with whole-brain connectivity patterns. *Cereb Cortex* 22:158–165
19. Yu Q, Erhardt EB, Sui J et al (2015) Assessing dynamic brain graphs of time-varying connectivity in fMRI data: application to healthy controls and patients with schizophrenia. *NeuroImage* 107:345–355
20. Zalesky A, Breakspear M (2015) Towards a statistical test for functional connectivity dynamics. *NeuroImage* 114:466–470
21. Leonardi N, Van De Ville D (2015) On spurious and real fluctuations of dynamic functional connectivity during rest. *NeuroImage* 104:430–436
22. Damaraju E, Allen EA, Belger A et al (2014) Dynamic functional connectivity analysis reveals transient states of dysconnectivity in schizophrenia. *Neuroimage Clin* 5:298–308
23. Du Y, Pearson GD, Yu Q et al (2016) Interaction among subsystems within default mode network diminished in schizophrenia patients: a dynamic connectivity approach. *Schizophr Res* 170:55–65
24. Fox MD, Snyder AZ, Vincent JL, Corbetta M, Van Essen DC, Raichle ME (2005) The human brain is intrinsically organized into dynamic, anticorrelated functional networks. *Proc Natl Acad Sci U S A* 102:9673–9678
25. Lin WC, Hsu TW, Chen CL et al (2012) Connectivity of default-mode network is associated with cerebral edema in hepatic encephalopathy. *PLoS One* 7:e36986
26. Qi R, Zhang LJ, Luo S et al (2014) Default mode network functional connectivity: a promising biomarker for diagnosing minimal hepatic encephalopathy: CONSORT-compliant article. *Medicine (Baltimore)* 93:e227
27. Iversen P, Sorensen M, Bak LK et al (2009) Low cerebral oxygen consumption and blood flow in patients with cirrhosis and an acute episode of hepatic encephalopathy. *Gastroenterology* 136:863–871
28. Chen HJ, Zhu XQ, Shu H et al (2012) Structural and functional cerebral impairments in cirrhotic patients with a history of overt hepatic encephalopathy. *Eur J Radiol* 81:2463–2469
29. Guevara M, Baccaro ME, Gomez-Anson B et al (2011) Cerebral magnetic resonance imaging reveals marked abnormalities of brain tissue density in patients with cirrhosis without overt hepatic encephalopathy. *J Hepatol* 55:564–573
30. Shakil S, Lee CH, Keilholz SD (2016) Evaluation of sliding window correlation performance for characterizing dynamic functional connectivity and brain states. *NeuroImage* 133:111–128